Human Interleukin 4 Receptor Complex: Neutralization Effect of Two Monoclonal Antibodies

S. Shane Taremi, Winifred W. Prosise, Nithya Rajan, Rosemary A. O'Donnell, and Hung V. Le*

Schering-Plough Research Institute, Kenilworth, New Jersey 07033

Received July 27, 1995; Revised Manuscript Received November 15, 1995[⊗]

ABSTRACT: The interaction of human interleukin 4 with the extracellular domain of its receptor α-subunit (shuIL-4Rα) was characterized in studies utilizing chemical cross-linking, size exclusion chromatography, and Western blot analysis. A 1:1 stoichiometric complex could be demonstrated over a wide range (0.04−2.7) of ligand−receptor concentration ratios. It could also be cross-linked with bifunctional reagents containing a minimum chain length of eight methylene residues or the equivalent (11.4 Å). Using surface plasmon resonance, (SPR) technology, we established the high-affinity of human interleukin 4 (huIL-4) to shuIL-4Rα which was immobilized on a BIAcore sensor chip (K_d = 46 pM). The mechanisms of action of neutralizing monoclonal antibodies (Mab) 25D2 and 35F2 [Abrams et al. (1991) U.S. Patent 5,041,381; Ramanathan et al. (1990) in *Advances in Gene Technology: The Molecular Biology of Immune Diseases and the Immune Response* (Streilein, J. W., et al., Eds.) p 163, IRL Press, Oxford; DeKruyff et al. (1989) *J. Exp. Med. 170*, 1477−1493] were subsequently evaluated on the basis of their interaction with huIL-4 in the presence of shuIL-4Rα. SPR studies showed that Mab 25D2 binds to huIL-4 and reduces its affinity for shuIL-4Rα by 54-fold. Formation of a ternary complex between Mab 25D2 and the huIL-4/shuIL-4Rα complex was demonstrated in size exclusion chromatography experiments. In contrast, Mab 35F2 which also binds huIL-4 failed to form a stable ternary complex with huIL-4 and shuIL-4Rα during size exclusion chromatography. SPR studies supported this finding and showed that the interactions of Mab 35F2 and shuIL-4Rα to huIL-4 are mutually exclusive. These data are consistent with results of previous epitope mapping studies showing that Mabs 25D2 and 35F2 bind to huIL-4 at two different sites [Ramanathan et al. (1993) *Biochemistry 32*, 3549−3556]. Together, the results suggest that Mab 25D2 binds to a domain in huIL-4 including helix D and exerts its inhibitory effect through a dual action. It decreases the affinity of huIL-4 for huIL-4Rα and potentially blocks interaction with a secondary receptor subunit such as the IL-2Rγ [Reusch et al. (1994) *Eur. J. Biochem. 222*, 491−499]. Mab 35F2 operates through a direct and simpler mechanism, binding to helix C and inhibiting huIL-4 activity by sterically excluding all interaction with huIL-4Rα.

Human interleukin 4 (huIL-4)[1] is a pleiotropic cytokine secreted by T lymphocytes, mast cells, and basophils (Paul, 1991). Some of its most recognizable functions include the ability to enhance expression of class II major histocompatibility antigens and the low-affinity receptor for IgE (CD23) on B cells (Rousset et al., 1988; Defrance et al., 1987a) and monocytes (Littman et al., 1989; te Velde et al., 1988), as well as the ability to induce antibody class switching to IgG1, IgM, and IgE in B lymphocytes (Pene et al., 1988). It is also a well-known growth regulator of T cells and B cells (Spits et al., 1987; Defrance et al., 1987b) and potentially of mast cells (Mosmann et al., 1986). All the biological functions of huIL-4 are mediated through a single class of high-affinity receptors exhibiting dissociation constants in the picomolar range (76−205 pM), in a wide variety of hematopoietic and nonhematopoietic cells (Cabrillat et al., 1987; Park et al., 1987). Molecular-cloning experiments first identified an α-receptor chain (huIL-4Rα) (Izerda et al., 1990; Galizzi et al., 1990) which binds huIL-4 with high affinity. However, subsequent studies pointed to the existence of a second receptor chain identical to the γ-chain of human interleukin 2 receptor (huIL-2Rγ) (Russell et al., 1993; Kondo et al., 1993). Both receptor chains belong to the cytokine receptor superfamily (Bazan, 1990; Takeshita et al., 1992). These findings were consistent with the current understanding of functional receptors for cytokines, which generally are comprised of several subunits contributing to either recognition or signal transduction.

Elucidation of the molecular basis of the interaction of huIL-4 with its functional cell surface receptor could provide a model for understanding specificity in cytokine recognition and signal transduction. Accordingly, the three-dimensional structure of huIL-4 was recently solved by NMR and X-ray crystallography (Powers et al., 1992; Garrett et al., 1992; Smith et al., 1992; Cook et al., 1991; Walter et al., 1992; Wlodawer et al., 1992). It is a canonical cytokine structure

* To whom correspondence should be addressed.

[⊗] Abstract published in *Advance ACS Abstracts,* February 1, 1996.

[1] Abbreviations: shuIL-4Rα, extracellular domain of the human interleukin 4 receptor α-subunit; huIL-4, human interleukin 4; IL-2Rγ, γ-subunit of interleukin 2 receptor; Mab, monoclonal antibody; SDS, sodium dodecyl sulfate; PAGE, polyacrylamide gel electrophoresis; BS^3; bis(sulfosuccinimidyl) suberate; DMA, dimethyl adipimidate·HCl; sulfo DST, disulfosuccinimidyl tartarate; sulfo EGS, ethylene glycol bis-(sulfosuccinimidyl succinate); DTSSP, 3,3′-dithiobis(sulfosuccinimidyl propionate); CHO, Chinese hamster ovary; HEPES, *N*-(2-hydroxyethyl)-piperazine-*N*′-2-ethanesulfonic acid; NHS, *N*-hydroxysuccinimide; EDC, *N*-ethyl-*N*′-[(dimethylamino)propyl]carbodiimide; BCIP/NBT, 5-bromo-4-chloro-3-indolyl phosphate/nitroblue tetrazolium; NHS-LC-biotin, sulfosuccinimidyl 6-(biotinamido)hexanoate; SPR, surface plasmon resonance; RU, resonance unit; P20, Tween-20; EDTA, ethylenediaminetetraacetic acid.

0006-2960/96/0435-2322$12.00/0

composed of four α-helices arranged in an up-up-down-down topology and connected by long loops which include two short antiparallel β-strands. Preliminary epitope mapping studies based on mutagenesis and immunochemical experiments (Ramanathan et al., 1993; Le et al., 1991; Kruse et al., 1993; Reusch et al., 1994) have implicated certain amino acid residues in helices A, C, and D as being critical for receptor interaction. These preliminary results provided the impetus for X-ray crystallography studies of the structures of shuIL-4Rα and shuIL-2Rγ and potentially the heterotrimeric complex of these two subunits with huIL-4 (Hoffman et al., 1995).

The availability of recombinant huIL-4 and soluble huIL-4 receptor complexes provides an excellent opportunity for design of antagonist-screening assays or for the characterization of clinically relevant monoclonal antibodies which act at the receptor level. In this report, we characterize the interaction between huIL-4 and shuIl-4Rα and utilize this system to establish the mechanism of action of anti-huIL-4 neutralizing monoclonal antibodies 25D2 and 35F2 (Abrams et al., 1991; Ramanathan et al., 1990; DeKruyff et al., 1989). It was previously demonstrated that both Mabs 35F2 and 25D2 (Ramanathan et al., 1993) bound to huIL-4 at two distinct sites in the four-α-helix structure. We now show that they block the action of huIL-4 by two different mechanisms. We also discuss the significance of these observations in relation to the epitopes, in huIL-4, recognized by the functional receptor complex. Understanding the mechanism of neutralization by these antibodies provides a rational basis for selection of candidates for humanization and potential clinical evaluation. This work was reported, in part, at the 1993 Protein Society annual meeting (Taremi et al., 1993).

EXPERIMENTAL PROCEDURES

Reagents. Prestained and unstained molecular mass markers for SDS−PAGE were purchased from BioRad and Pharmacia, respectively. Molecular mass markers for size exclusion chromatography were purchased from Pharmacia. The cross-linking reagents BS^3, DMA, sulfo DST, sulfo EGS, and DTSSP were purchased from Pierce Chemical Co. (Rockford, IL). Anti-huIL-4 rat monoclonal antibodies 25D2 and 35F2 were obtained as previously described (Ramanathan et al., 1993). P71 is a rabbit antiserum to NS1-derived shuIL-4Rα.

Recombinant huIL-4 expressed CHO cells or *Escherichia coli* was purified to homogeneity with a final specific activity of 2×10^7 units/mg as previously described (Le et al., 1988; Tang et al., 1991). Recombinant shuIL-4Rα was purified from CHO cell supernatants by a combination of ion exchange and immunoaffinity chromatography as described elsewhere (Rajan et al., 1995). Recombinant shuIL-4Rα was also expressed in NS1 cells and purified from cell supernatant in a single step, using a huIL-4 affinity column (Izerda et al., 1990). shuIL-4Rα, purified from either cell line, was greater than 95% pure as determined by N-terminal sequencing and SDS−PAGE.

Biotinylation of CHO-Derived huIL-4Rα. CHO-derived shuIL-4Rα (0.5 mg) in 1 mL of 50 mM sodium phosphate buffer (pH 7.6) and 150 mM NaCl was biotinylated by the addition of a 5 M excess of NHS-LC-biotin (Pierce). After a 3 h incubation at room temperature, 1.0 mL of 1.0 M ethanolamine (pH 9.0) was added and the mixture was further incubated for 1 h at room temperature. The excess biotin and ethanolamine was removed by dialysis against 4 L of PBS [50 mM sodium phosphate (pH 7.6), 150 mM NaCl, and 1 mM EDTA]. The sample was finally concentrated to 2.0 mg/mL on a Centricon-10 concentrator (Amicon, Beverly, MA).

Cross-Linking. Cross-linking reactions were performed at room temperature in a final volume of 30 μL, in 50 mM sodium phosphate buffer (pH 7.8). In a typical experiment, huIL-4 and shuIL-4Rα were allowed to incubate for 1 h at room temperature. The cross-linking reagent was then added to a final concentration of 1 mM, from stock solutions, freshly prepared in 50 mM phosphate buffer (pH 7.8). The final concentration of huIL-4 and shuIL-4Rα was maintained at 1 μM. Following an additional 30 min incubation, the reaction was terminated by the addition of 1.0 M Tris (pH 7.6) to a final concentration of 100 mM. The mixture was then immediately prepared for SDS−PAGE by the addition of 30 μL of SDS sample buffer (250 mM Tris-HCl, 2% SDS, 10% β−mercaptoethanol, and 30% glycerol).

Size Exclusion Chromatography. NS1-derived shuIL-4Rα and CHO-derived huIL-4 were incubated for 2 h at 4 °C in 50 mM sodium phosphate buffer (pH 7.6), 200 mM NaCl, and 1 mM EDTA at a 1:1 molar ratio. The concentration of huIL-4 was kept at 20 μM (0.3 mg/mL). Samples (200 μL) were applied to a Superdex-75 HR (1 × 30 cm) FPLC column (Pharmacia, Piscataway, NJ) equilibrated with sample buffer. The column was calibrated using molecular mass standards (bovine serum albumin, 67 kDa; ovalbumin, 43 kDa; chymotrypsinogen A, 25 kDa; ribonuclease A, 13.7 kDa), CHO-derived huIL-4, and NS1-derived shuIL-4Rα. Flow rate was maintained at 0.5 mL/min, and protein elution was monitored spectrophotometrically at 280 nm.

Mixtures of CHO-derived huIL-4, NS1-derived, shuIL-4Rα, and monoclonal antibodies were analyzed in a similar manner, using a Superose-12 HR (1 × 30 cm) FPLC column. NS1-derived shuIL-4Rα, CHO-derived huIL-4, and either Mab 35F2 or Mab 25D2 were incubated in an equimolar concentration (2.0:2.0:2.0 μM) for 2 h at 4 °C in 50 mM sodium phosphate buffer (pH 7.6), 200 mM NaCl, and 1 mM EDTA. The samples (50 μL) were then applied to columns, equilibrated in sample buffer, and calibrated with molecular mass standards (catalase, 232 kDa; aldolase, 158 kDa; bovine serum albumin, 67 kDa; ovalbumin, 43 kDa; chymotrypsinogen A, 25 kDa; ribonuclease A, 13.7 kDa), CHO-derived huIL-4, NS1-derived shuIL-4Rα, Mab 35F2, and Mab 25D2. Further calibrations were also performed with binary complexes of huIL-4 and shul-L4Rα and Mab 25D2 and Mab 35F2, respectively. Flow rate was maintained at 0.5 mL/min, and protein elution was monitored at 280 nm.

Surface Plasmon Resonance Measurements. The molecular interactions between *E. coli*-derived huIL-4, CHO-derived shuIL-4Rα, and anti-huIL-4 monoclonal antibodies 25D2 and 35F2 were determined by surface plasmon resonance measurements using the BIAcore instrument (Pharmacia Biosensor, Piscataway, NJ) described in detail elsewhere (Karlsson et al., 1991; Johnsson et al., 1991). All ligands (CHO-derived shuIL-4Rα, Mab 25D2, Mab 35F2, and streptavidin) were immobilized on a sensor chip surface using reagents in the amine-coupling kit provided by the manufacturer, with slight modifications of the available

procedure. The eluent buffer was 50 mM HEPES (pH 7.4), 0.15 M NaCl, 3.4 mM EDTA, and 0.005% P20. All experiments were carried out at 25 °C and at a flow rate of 5 μL/min or as otherwise indicated. The conversion of resonance units (RU) to surface concentration of proteins (in molarity) in all cases was determined from conversion factors which were previously determined by Stenberg et al. (1991): 1000 RU = 1 ng/mm^2 = 1 ng/0.000 12 mm^3 (since the thickness of the matrix is 0.000 12 mm) = 8.3 g/L. Molar concentrations of immobilized proteins were deduced from their molecular masses. Kinetic constants for the various interactions were determined according to methodology previously described (Karlsson et al., 1991), using Pharmacia BIAlogue Kinetics Evaluation Software. Briefly, the association of an analyte to the surface-immobilized ligand is described by $dR/dt = k_{on}CR_{max} - (k_{on}C + k_{off})R_{t_n}$, where k_{on} is the association rate constant, C is the concentration of analyte, R_{max} is the maximum binding capacity of the ligand, k_{off} is the dissociation rate constant, and R_{t_n} is the amount of analyte bound to the ligand at time t_n. A plot of dR/dt vs R_{t_n} gives a line with slope $k_s = -(k_{on}C + k_{off})$. A plot of k_s vs C for various concentrations of analyte results in a slope of the fitted line which is equal to k_{on}.

The dissociation rate constant, k_{off}, is determined by the first order rate equation $dR/dt = k_{off}R_{t_n}$, measured when analyte passing over the ligand is replaced with buffer and under the conditions where R approaches R_{max} to minimize the effect of rebinding. k_{off} is obtained from the slope of the $\ln(R_{t_1}-R_{t_n})$ vs t plot during the initial phase of dissociation (first 60 s), where R_{t_1} is the amount of bound analyte at time t_1, R_{t_n} is the amount of bound analyte at time t_n, and t is $t_n - t_1$. The equilibrium dissociation constant is $K_d = k_{off}/k_{on}$.

HuIL-4 and shuIL-4Rα Interaction. The carboxymethylated dextran surface of a sensor chip was modified with streptavidin first by activation of the surface with a 15 μL injection of NHS/EDC. This was followed by an injection of 30 μL of streptavidin at 0.4 mg/mL in 10 mM sodium aceate (pH 4.0). The remaining activated esters were blocked by injection of 30 μL of 1 M ethanolamine. These conditions resulted in 2400 RU of streptavidin, immobilized on the sensor chip. Coupling of shuIL-4Rα to the streptavidin surface was accomplished by injection of 30 μL of biotinylated shuIL-4Rα (30 μg/mL) in 50 mM sodium phosphate (pH 7.6), 150 mM NaCl, and 1 mM EDTA. The procedure consistently resulted in 950 RU of bound receptor. For kinetic analysis, 30 μL samples of *E. coli*-derived huIL-4 at several concentrations (2.5, 5, 7, 10, and 15 nM) were injected over the biotinylated shuIL-4Rα-modified surface at 10 μL/min. The dissociation rate constant was determined using the dissociation phase of a sensorgram collected using a two-step methodology: (1) injection of 40 μL of *E. coli* huIL-4 at 300 nM, previously determined to saturate all the immobilized shuIL-4Rα, followed by (2) injection of 40 μL of shuIL-4Rα at 1 μM during the dissociation phase to minimize rebinding of huIL-4 to the shuIL-4Rα surface. The sensor chip was regenerated between each run with a 1 min pulse of 10 mM HCl, at 5 μL/min. The effect of anti-huIL-4 antibodies was determined by injection of 35 μL of a mixture of *E. coli*-derived huIL-4 and Mab 35F2 or 25D2 dissolved in HBS buffer containing 0.005% P20. The concentration of huIL-4 (0.66 μM) in the mixture was kept at a saturating level with respect to the concentration of receptor immobilized on the sensor chip. The concentration of antibody was maintained at 2 μM.

HuIL-4 and Monoclonal Antibody Interactions. The affinities between huIL-4 and either Mab 25D2 or Mab 35F2 were determined in separate experiments. The sensor chip was activated with a 10 μL injection of NHS/EDC, followed by an injection of 35 μL of *E. coli*-derived hu-IL4 at 30 μg/mL in 10 mM sodium acetate (pH 5.0). The remaining activated esters were blocked by injection of 30 μL of 1 M ethanolamine. These conditions resulted in 639 RU, corresponding to 354 μM huIL-4, immobilized on the chip. For kinetic analysis, 40 μL of either Mab 25D2 or Mab 35F2 at various concentrations (67, 100, 133, 167, 200, 233, 267, and 300 nM) in HBS was injected over the huIL-4-modified surface at 10 μL/min. The sensor chip was regenerated between each run with a 1 min pulse of 100 mM HCl, at 10 μL/min.

ShuIL-4Rα/huIL-4-25D2 Complex Interaction. A sensor chip was activated with a 10 μL injection of NHS/EDC, followed by an injection of 35 μL of Mab 25D2 at 0.1 mg/mL in 10 mM sodium acetate (pH 4.0). The remaining activated esters were blocked by an injection of 35 μL of 1 M ethanolamine. These conditions resulted in 2918 RU, corresponding to 163 μM Mab 25D2, immobilized on the sensor chip. For kinetic analysis, five samples each comprised of a 35 μL injection of *E. coli*-derived huIL-4 (2 μM) followed immediately by 35 μL aliquots of CHO-derived shuIL-4Rα at various concentrations (21, 42, 126, 210, and 295 nM) were injected over the sensor chip at 10 μL/min in HBS buffer containing 0.005% P20. The sensor chip was regenerated between each run with a 1 min pulse of 100 mM HCl, at 10 μL/min.

Protein Sequencing. N-terminal protein sequencing was performed on an Applied Biosystems model 477A protein sequencer equipped with on-line high-performance liquid chromatography (HPLC) analysis of PTH amino acids. Standard reaction and conversion cycles were used as suggested by the manufacturer.

Electrophoresis and Immunoblotting. SDS−PAGE was performed with precast 10 to 20% gradient gels purchased from Integrated Separation Systems (Natick, MA). Proteins from the gel were electroblotted onto a nitrocellulose membrane using a semidry transfer apparatus obtained from the same manufacturer. Immunodetection of shuIL-4Rα was accomplished with P71 rabbit polyclonal antibody (1:1000 dilution in 1% BSA), followed by development with biotin-labeled goat anti-rabbit (H + L) IgG (Jackson Immunochemicals, West Grove, PA) at a 1:25000 dilution and streptavidin alkaline phosphatase (GIBCO/BRL, Gaithersburg, MD) at a 1:5000 dilution. Immunodetection of huIL-4 was accomplished with rat Mab 25D2 at 1 μg/mL in the presence of 1% BSA, followed by incubation with alkaline phosphatase-conjugated goat anti-rat IgG (Jackson Immunochemicals). Between each incubation, the blots were washed with 50 mM Tris (pH 7.4) and 0.15 M NaCl containing 0.05% Tween-20 for 15 min. BCIP/NBT (Kirkegaard & Perry, Gaithersburg, MD) was used as substrate for the color development of all blots.

Protein Determination. The concentrations of huIL-4 and shuIL-4Rα were determined spectrophotometrically using the extinction coefficients ${}^{0.1\%}E_{280\ nm} = 0.625$ mg^{-1} cm^2 (Windsor et al., 1991) and ${}^{0.1\%}E_{280\ nm} = 2.72$ mg^{-1} cm^2 (Rajan et al., 1995), respectively. The concentrations of the anti-huIL-4

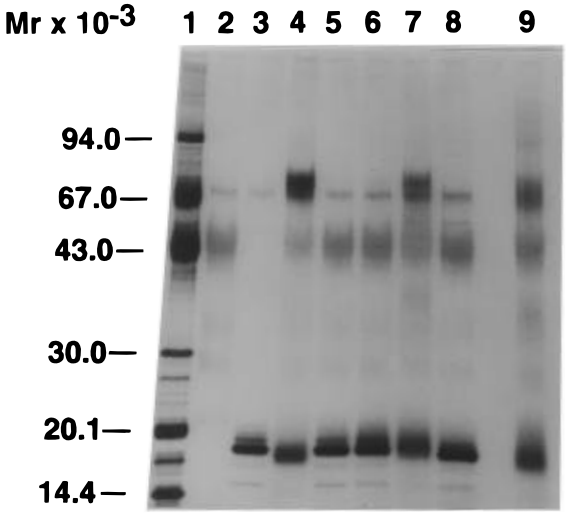

FIGURE 1: SDS−PAGE of cross-linked huIL-4/shuIL-4Rα complex. CHO-derived huIL-4 (1 μM) was incubated with NS1-derived shuIL-4Rα (1 μM) in 50 mM sodium phosphate buffer (pH 7.8) in the presence of various homobifunctional NHS esters (1 mM). After 30 min, the reaction was quenched with 0.1 M Tris (pH 7.8). Small aliquots were subjected to SDS−PAGE (10 to 20% polyacrylamide gradient) and stained with silver. Lanes: (1) molecular mass standards (phosphorylase *b*, 94.0 kDa; bovine serum albumin, 67 kDa; ovalbumin, 43 kDa; carbonic anhydrase, 30 kDa; soybean trypsin inhibitor, 20.1 kDa; α-lactalbumin, 14.1 kDa); (2) NS1-derived shuIL-4Rα; (3) CHO-derived huIL-4; (4−7) CHO-derived huIL-4 and NS1-derived shuIL-4Rα treated with BS^3, DMA, sulfo DST, and sulfo EGS, respectively; (8 and 9) CHO-derived huIL-4 and NS1-derived shuIL-4Rα treated with DTSSP in the presence and absence of β-mercaptoethanol, respectively.

monoclonal antibodies were determined spectrophotometrically using the extinction coefficient ${}^{0.1\%}E_{280\ nm} = 1.35\ mg^{-1}\ cm^2$ (Little & Donuahue, 1967).

RESULTS

Cross-Linking of huIL-4 to shuIL-4Rα. The interaction of huIL-4 and shuIL-4Rα was first investigated in cross-linking studies. Five different water soluble bifunctional reagents of various lengths, sulfo DST (6.4 Å), DMA (8.6 Å), BS^3 (11.4 Å), DTSSP (12 Å), and sulfo EGS (16.1 Å), were employed in a study involving NS1-derived shuIL-4Rα and CHO-derived huIL-4. Figure 1 shows that the addition of excess BS^3, sulfo EGS, and DTSSP (lanes 4, 7, and 9) to an equimolar mixture of huIL-4 and shuIL-4Rα resulted in the formation of a new species with an apparent M_r of 80 000 detected by SDS−PAGE. The same 80 000 M_r species obtained by cross-linking with DTSSP was not present when the reaction mixture was treated with reducing agent (lane 8) prior to electrophoresis. Neither huIL-4 nor shuIL-4Rα alone could be polymerized by these reagents in control experiments. Using BS^3 as a prototype, it was also demonstrated that varying reagent concentrations between 0.1 and 5 mM, or extending incubation time from 30 min to 2 h, did not produce additional M_r species that are detectable by SDS−PAGE. The cross-linking studies further established that treatment of the mixture of huIL-4 and shuIL-4Rα with DMA and sulfo DST did not result in the formation of the 80 000 M_r species. This observation suggested that the length of the bifunctional reagents was critical and that successful cross-linking requires a minimum chain length equivalent to eight methylene residues or 11.4 Å (i.e. the chain length of BS^3).

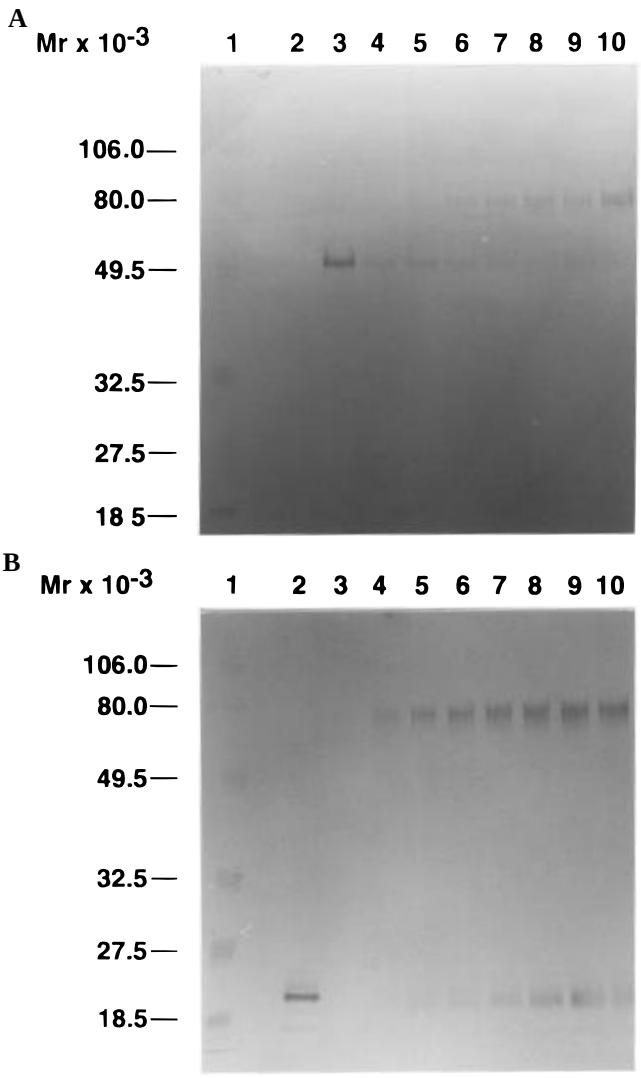

FIGURE 2: Detection of the huIL-4/shuIL-4Rα complex by Western blots. NS1-derived shuIL-Rα (1 μM) was incubated with increasing concentrations of CHO-derived huIL-4 in 50 mM sodium phosphate (pH 7.8) in the presence of 1 mM BS^3 for 1 h at room temperature. Small aliquots from the reaction mixtures were subjected to SDS−PAGE as described in Figure 1. Proteins from the gel were electroblotted onto nitrocellulose for immunodetection with either rabbit antiserum (P71) to shuIL-4Rα (panel A) or a monoclonal antibody (25D2) to huIL-4 (panel B). Application of conjugated antibodies and color development was performed as described in Experimental Procedures. Lanes: (1) prestained molecular mass standards (phosphorylase *b*, 106 kDa; bovine serum albumin, 80 kDa; ovalbumin, 49.5 kDa; carbonic anhydrase, 32.5 kDa; soybean trypsin inhibitor, 27.5 kDa; lysozyme, 18.5 kDa); (2) CHO-derived huIL-4 (3.2 μM); (3) NS1-derived shuIL-Rα (1 μM); (4−10) 1 μM NS1-derived shuIL-4Rα incubated with 1 mM BS^3 and 0.04, 0.4, 0.9, 1.3, 1.8, 2.2, and 2.7 μM CHO-derived huIL-4, respectively.

Western blot studies of the 80 000 M_r species were performed with a monoclonal antibody to huIL-4 (Mab 25D2) and a polyclonal antiserum (P71) to shuIL-4Rα. Figure 2 shows that both huIL-4 and shuIL-4Rα could be detected in this complex when cross-linking with BS^3 was performed at different molar ratios of huIL-4 to shuIL-4Rα. The intensity of the Western-blotted 80 000 M_r species increased proportionally with an increasing molar ratio of huIl-4:shuIL-4Rα from 0.04 to 2.7, and the increase was independent of the primary antibody employed for detection of either huIL-4 or shuIL-4Rα. Moreover, additional species

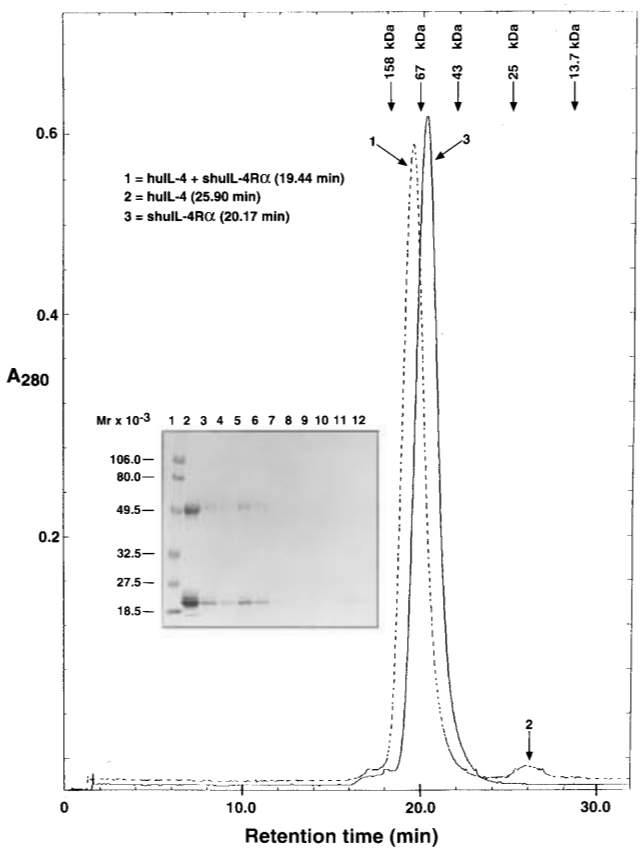

FIGURE 3: Size exclusion chromatography of the shuIL-4Rα/huIL-4 complex. NS1-derived shuIL-4Rα was chromatographed separately (—) and in an equimolar mixture with CHO-derived huIL-4 (- - -), on a Superdex 75 HR (1 × 30 cm) column. The column was equilibrated in 0.05 M sodium phosphate, 0.001 M EDTA, and 0.2 M NaCl (pH 7.6), and flow rate was maintained at 0.5 mL/min. Column effluent was monitored spectrophotometrically at 280 nm. Fractions obtained from chromatography of the mixture of huIL-4 and receptor were subjected to SDS−PAGE as shown in the inset. Lanes: (1) prestained molecular mass standards (phosphorylase *b*, 106 kDa; bovine serum albumin, 80 kDa; ovalbumin, 49.5 kDa; carbonic anhydrase, 32.5 kDa; soybean trypsin inhibitor, 27.5 kDa; lysozyme, 18.5 kDa); (2) equimolar mixture of NS1-derived shuIL-4Rα and CHO-derived huIL-4 (10 μg); (3) equimolar mixture of NS1-derived shuIL-4Rα and CHO-derived huIL-4 (1 μg); (4−7) eluted fractions corresponding to peak 1; (8−11) eluted fractions corresponding to peak 2. Arrows in the chromatogram indicate the retention times of molecular mass markers used during calibration.

with a M_r greater than 80 000 were not evident when either huIL-4 or shuIL-4Rα was present in excess. The available data indicate that only one cross-linked complex containing both huIL-4 and shuIL-4Rα could be obtained under these experimental conditions.

Size Exclusion Chromatography and Stoichiometry of the huIL-4/shuIL-4Rα Complex. The apparent M_r of the huIL-4/shuIL-4Rα complex was further evaluated by size exclusion chromatography. Figure 3 shows the elution profile of an equimolar mixture of NS1-derived shuIL-4Rα and CHO-derived huIL-4, which was chromatographed under identical conditions as a control sample containing only shuIL-4Rα. The chromatogram of the mixture reveals two well-resolved species, peaks 1 and 2, at retention times 19.44 and 25.90 min, respectively. The retention time for peak 2 corresponds exactly to that of CHO-derived huIL-4, which was chromatographed separately in calibration experiments (data not shown). The retention time of peak 1, corresponding to an apparent M_r of 74 000, could not be assigned to either CHO-derived huIL-4 or NS1-derived shuIL-4Rα. Furthermore, no additional peaks at smaller retention times (higher apparent molecular mass) than peak 1 were detected when the mixture of huIL-4 and shuIL-4Rα was chromatographed at a 1:10 molar ratio. SDS−PAGE analysis of fractions collected under peaks 1 and 2 is shown in the inset of Figure 3. Fractions corresponding to peak 2 (lanes 9−11) contain only CHO-derived huIL-4, whereas fractions corresponding to peak 1 contain both huIL-4 and shuIL-4Rα (lanes 4−7). Their relative amounts were estimated spectrophotometrically by scanning the coomassie-stained gel at 495 nm and using known amounts of the two proteins as standards. The results revealed a 1.2:1.0 huIL-4 to shuIL-4Rα stoichiometry. The presence of both huIL-4 and shuIL-4Rα in peak 1 was confirmed by ten cycles of N-terminal sequence analysis. Two distinct sequences, HK-DITLQEI and GNMKVLQEPT, were detected and could be assigned to the N-terminal amino acid residues of huIL-4 and shuIL-4Rα, respectively. PTH amino acid yields for the triplet LQE, which occurs in both sequences, were consistent with the occurrence of equimolar amounts of these two proteins in peak 1.

Size Exclusion Chromatography of huIL-4, shuIL-4Rα, and Monoclonal Antibody Complexes. An equimolar mixture of huIL-4, shuIL-4Rα, and Mab 25D2 was incubated for 2 h at room temperature and then chromatographed on a Superose 12 column. The resulting elution profile (Figure 4A) provided evidence for the separation of several species corresponding to huIL-4, Mab 25D2, and a complex of huIL-4 and Mab 25D2. However, an additional species with a higher apparent M_r than the complex of huIL-4 and Mab 25D2 was also observed (Figure 4A). SDS−PAGE analysis of the fractions corresponding to this novel species revealed the presence of huIL-4, Mab 25D2, and shuIL-4Rα (data not shown). A similar size exclusion chromatography study was performed with an equimolar mixture of huIL-4, shuIL-4Rα, and Mab 35F2 (Figure 4B). The resulting elution profile revealed only two major species corresponding to complexes of huIL-4 with either shuIL-4Rα or Mab 35F2.

Real-Time Interaction Studies. Binary and ternary complex formation between huIL-4, shuIL-4Rα, Mab 25D2, and Mab 35F2 was also analyzed in real time, using surface plasmon resonance (Fägerstam, 1991). The binding kinetics of huIL-4 to shuIL-4Rα immobilized onto a sensor chip is shown in Figure 5. Analysis of binding rate vs concentration of bound huIL-4 at various time points provides the basis for derivation of both the association rate constant of 7.75×10^6 M^{-1} s^{-1} and the dissociation rate constant of 3.58×10^{-4} s^{-1}. The calculated dissociation constant ($K_d = k_{off}/k_{on}$) was 46 pM. Figure 6 also shows the binding of huIL-4 to shuIL-4Rα immobilized on a sensor chip, performed after preincubation of huIL-4 with a 3-fold molar excess of either Mab 25D2 or 35F2. The results obtained were then compared to binding of huIL-4 alone to the immobilized shuIL-4Rα under identical conditions. It is notable that preincubation of huIL-4 with Mab 25D2 caused a 9-fold increase in RUs, whereas preincubation with Mab 35F2 inhibited binding of huIL-4 to the sensor chip. Since the resonance effect is directly proportional to the mass of bound components, the increment observed following preincubation with Mab 25D2 is a consequence of binding of Mab 25D2 to the shuIL-4Rα-immobilized surface. This binding is mediated by huIL-4 since Mab 25D2 applied at the same

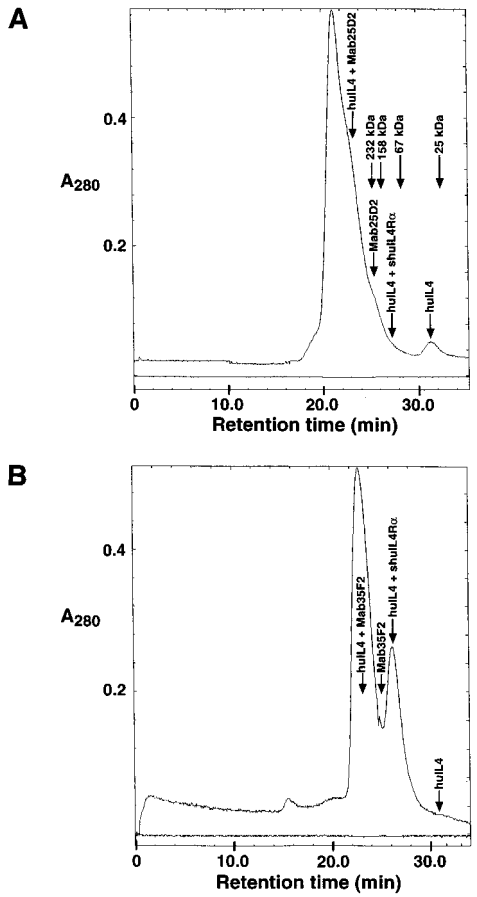

FIGURE 4: Size exclusion chromatography of huIL-4, shuIL-4Rα, and monoclonal antibody complexes. Chromatography was performed with a Superose 12 HR column (1 × 30 cm) equilibrated in 0.05 M sodium phosphate, 0.001 M EDTA, and 0.2 M NaCl (pH 7.6). Flow rate was maintained at 0.5 mL/min, and protein elution was monitored spectrophotometrically at 280 nm. The column was precalibrated as described in Experimental Procedures: (A) chromatogram of an equimolar mixture of CHO-derived huIL-4, NS1-derived shuIL-4Rα, and Mab 25D2; (B) chromatogram of an equimolar mixture of CHO-derived huIL-4, NS1-derived shuIL-4Rα, and Mab 35F2. Arrows in the chromatograms indicate the retention volumes of molecular mass standards and various marker proteins used for calibration.

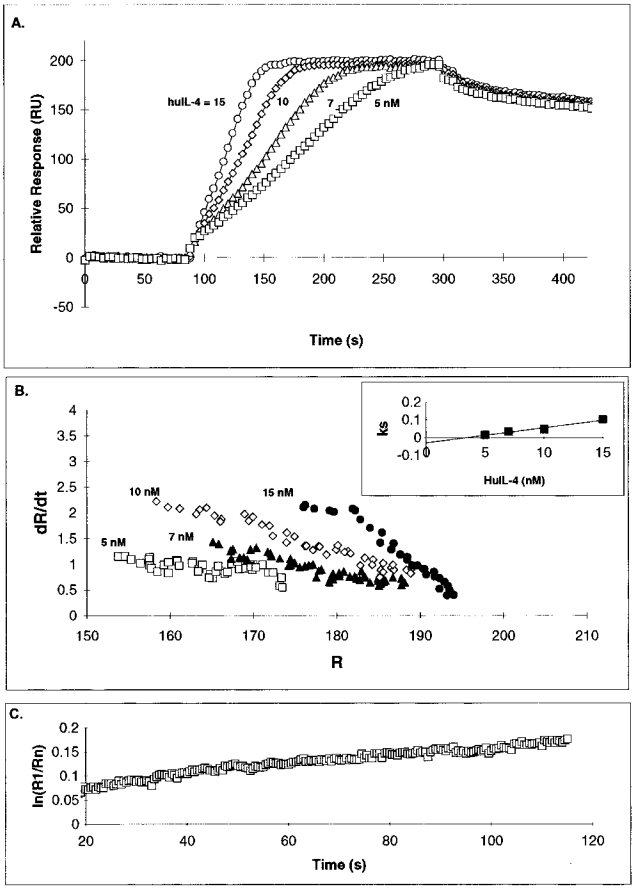

FIGURE 5: Kinetics of binding of huIL-4 to shuIL-4Rα immobilized on a BIAcore biosensor. (A) Biotinylated CHO-derived shuIL-4Rα was coupled at a level of 950 RU (corresponding to 330 μM) to a chip previously derivatized with streptavidin through standard amine chemistry. Aliquots (35 μL) at various concentrations of *E. coli*-derived huIL-4 (5−15 nM) were then injected over the sensor chip at 10 μL/min in HBS buffer containing 0.005% P20. (B) Calculation of the association rate constant. Association phases of IL-4 concentration binding curves at 15, 10, 7, and 5 nM where the binding is not limited by mass transport (corresponding kinetic data from 136−146, 154−172, 190−213, and 252−263 s, respectively) were used to plot the change in rate of binding vs time. The slope of these lines resulted in a k_s value at each concentration. The inset shows the plot of k_s vs concentration. The slope of the fitted line is the association rate constant, k_{on}. (C) Calculation of the dissociation rate constant. Due to the high association rate of this interaction and thus possible rebinding of huIL-4 during the dissociation phase, the dissociation rate constant was determined using the dissociation phase of a sensorgram collected using a two-step methodology as described in Experimental Procedures. The slope of the fitted line to the plot of $\ln(R_{t_1}-R_{t_n})$ vs t during the initial phase of dissociation (first 60 s) is the dissociation rate constant, k_{off}.

concentration in the absence of huIL-4 did not induce any increase in resonance effect (data not shown).

Effect of Mab 25D2 on the Binding Affinity of huIL-4 for shuIL-4Rα. Mab 25D2 and Mab 35F2 are known to be neutralizing and bind to huIL-4 with high affinity (Ramanathan et al., 1990, 1993; Abrams et al., 1991; DeKruyff et al., 1989). Determination of kinetic constants for the binding of huIL-4 to Mab 25D2 and 35F2 using surface plasmon resonance is summarized in Table 1. The association rates were comparable in magnitude, 1.02×10^5 and 2.78×10^5 M^{-1} s^{-1}, for Mab 25D2 and 35F2, respectively. However, the dissociation rate of Mab 25D2 was disproportionately slower (3.10×10^{-6} s^{-1}) in comparison to that of Mab 35F2 (3.24×10^{-4} s^{-1}). As a result, the calculated dissociation constants based on these determinations were notably different for Mab 25D2 ($K_d = 3.04 \times 10^{-11}$ M) and Mab 35F2 ($K_d = 1.16 \times 10^{-9}$ M).

The affinity of shuIL-4Rα for the huIL-4/Mab 25D2 complex was evaluated as shown in Figure 7, taking advantage of the very slow dissociation rate and high affinity of Mab 25D2. Analysis of binding rate vs concentration of bound shuIL-4Rα at various times allows for calculation of the kinetic rates constants and dissociation constant summarized in Table 1. The dissociation constant (K_d) for shuIL-4Rα bound to huIL-4 complexed with Mab 25D2 was calculated to be 2.50×10^{-9} M. This value is 54-fold larger than observed for the binding for huIL-4 to shuIL-4Rα immobilized to a sensor chip, indicating that binding of Mab 25D2 to huIL-4 decreases binding affinity for shuIL-4Rα by more than 1 order of magnitude.

DISCUSSION

The experiments reported in this study provide a preliminary analysis of the interaction between highly purified

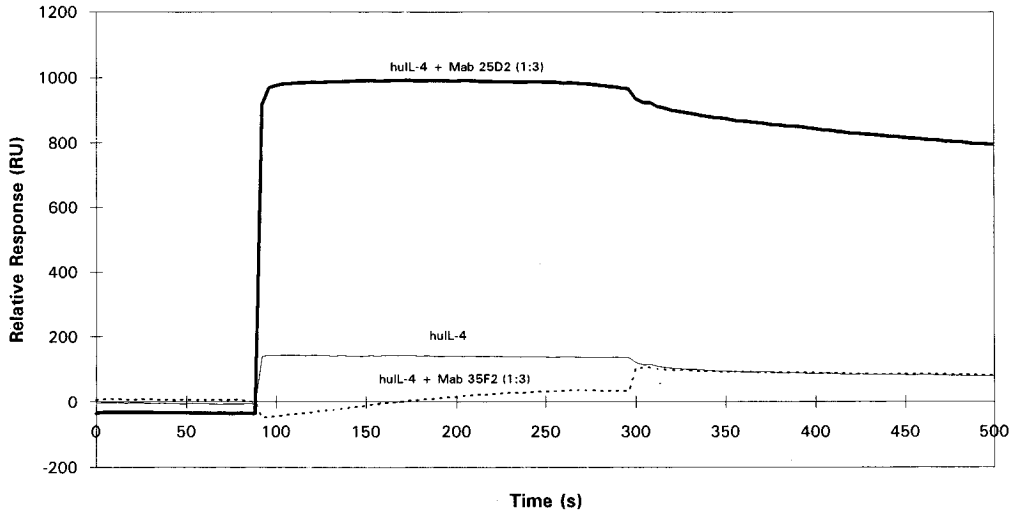

FIGURE 6: Surface plasmon resonance studies of the interaction of huIL-4 with shuIL-4Rα in the presence of Mab 25D2 and Mab 35F2. Biotinylated CHO-derived shuIL-4Rα was coupled at a level of 1100 RU (corresponding to 385 μM) to a biosensor chip previously derivatized with streptavidin through standard amine chemistry. Aliquots (35 μL) of *E. coli*-derived huIL-4 (0.66 μM) (light line), a mixture of *E. coli*-derived huIL-4 (0.66 μM) and Mab 25D2 (2 μM) (bold line), or a mixture of *E. coli*-derived huIL-4 (0.66 μM) and Mab 35F2 (2 μM) (dotted line) were injected over the biosensor chip at 10 μL/min in HBS buffer containing 0.005% P20. The small downward deflections observed at the beginning (90 s) and the end of the injection (300 s) of the huIL-4 and Mab 35F2 mixture is due to a slight difference in buffer composition of the sample and BIAcore running buffer.

Table 1: Kinetic Constants for Interaction of huIL-4 with shuIL-4Rα and Anti-IL-4 Monoclonal Antibodies

immobilized ligand	analyte	k_{on} (M^{-1} s^{-1})[a]	k_{off} (s^{-1})[a]	K_d (M)[b]
shuIL-4Rα	huIL-4	$(7.75 \pm 1.8) \times 10^6$	$(3.58 \pm 0.02) \times 10^{-4}$	$(4.62 \pm 0.12) \times 10^{-11}$
huIL-4	Mab 25D2	$(1.02 \pm 0.21) \times 10^5$	$(3.10 \pm 0.17) \times 10^{-6}$	$(3.04 \pm 0.80) \times 10^{-11}$
huIL-4	Mab 35F2	$(2.78 \pm 0.14) \times 10^5$	$(3.24 \pm 0.33) \times 10^{-4}$	$(1.16 \pm 0.23) \times 10^{-9}$
Mab 25D2/huIL-4[c]	shuIL-4Rα	$(4.30 \pm 0.13) \times 10^5$	$(1.08 \pm 0.01) \times 10^{-3}$	$(2.50 \pm 0.35) \times 10^{-9}$

[a] On-rate and off-rate constants were measured at 25 °C as described in Experimental Procedures. [b] Calculated from k_{off}/k_{on} for each experiment. [c] Mab 25D2 was immobilized onto a sensor chip and was used as a capture antibody for huIL-4.

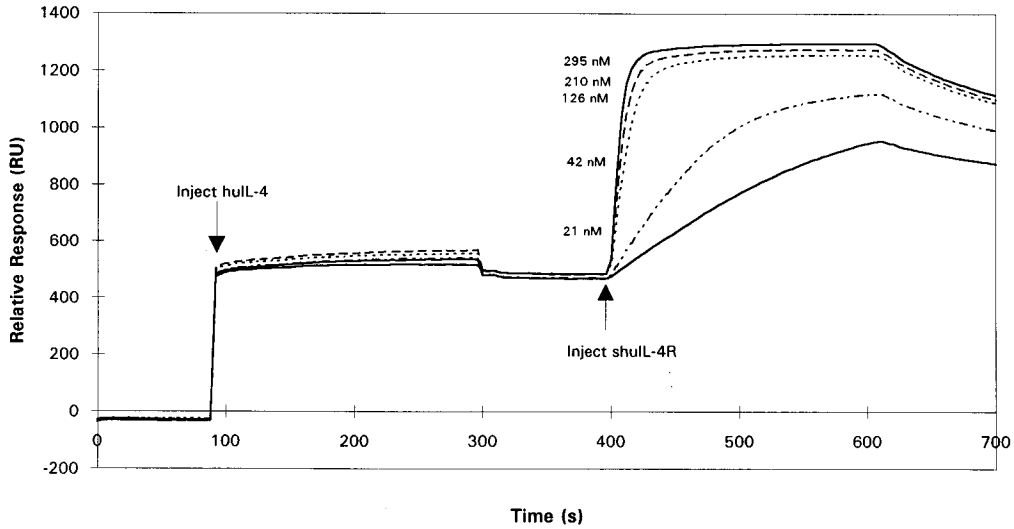

FIGURE 7: Kinetics of binding of shuIL-4Rα to a complex of huIL-4 and Mab 25D2 immobilized on a BIAcore biosensor. Mab 25D2 was coupled at a level of 2900 RU (corresponding to 160 μM) to a biosensor chip through standard amine chemistry. Aliquots of 35 μL of *E. coli*-derived huIL-4 (2 μM) were injected over the sensor chip at 10 μL/min in HBS buffer containing 0.005% P20, followed immediately by a 100 s wash period and an additional 35 μL aliquot of CHO-derived shuIL-4Rα at various concentrations (21, 42, 126, 210, and 295 nM). The association rate constant for the interaction of shuIL-4Rα and Mab 25D2-bound huIL-4 was determined from the association phase of the curves collected from 400 to 600 s.

huIL-4 and shuIL-4Rα. This cytokine/receptor complex was then employed in experiments designed to establish the molecular basis of the neutralization mechanisms of huIL-4 by the two monoclonal antibodies, 35F2 and 25D2, which have been targeted for humanization and potential clinical applications (Abrams et al., 1993). These studies demonstrate that monoclonal antibodies 35F2 and 25D2 neutralize huIL-4 through distinct mechanisms and provide further insight about the domains in huIL-4 that are available for interaction with functional receptors in responsive cells.

Analysis of the complex of huIL-4 and shuIL-4Rα, chemically cross-linked with BS^3, clearly indicates the presence of only one complex with an apparent M_r of 80 000, corresponding to one molecule of huIL-4 and one molecule

of shuIL-4Rα. This 1:1 stoichiometry was demonstrated by isolation of the pure complex by size exclusion chromatography and direct determination of its composition by SDS−PAGE, protein concentration determination, amino acid sequencing, and Western blotting with appropriate antibodies (Figures 2 and 3). Successful cross-linking between huIL-4 and shuIL-4Rα requires the use of bifunctional reagents containing a minimum chain length of 11.4 Å. This observation is of particular interest since it provides preliminary information about the proximity of reactive side chains located at, or near, the respective binding domains of the huIL-4/shuIL-4Rα complex. K_{84} in huIL-4 is an excellent candidate for cross-linking with a reactive side chain in the binding domain of shuIL-4Rα. Mutagenesis studies have already shown that K_{84} is essential for receptor binding and T cell proliferation (Ramanathan et al., 1993). It is also in close proximity to R_{88} which has been directly implicated in the binding of huIL-4 to shuIL-4Rα. Our results are consistent with the preliminary native gel electrophoresis and gel filtration studies reported by Hoffman et al. (1995). The stoichiometric complex was the only molecular weight species ($M_r \sim 80\,000$) formed when shuIL-4Rα was mixed with huIL-4 over a wide range of concentration ratios. Hence, homodimerization or oligomerization of shuIL-4Rα induced by receptor occupancy was not observed.

Using SPR technology, we studied the interaction of huIL-4 with shuIL-4Rα immobilized on a sensor chip. The kinetics of association and dissociation followed the predicted model for monovalent and noncooperative ligand−receptor interaction (Karlsson et al., 1991). At 25 °C, the interaction was characterized by a high association rate of $k_{on} = 7.75 \times 10^6\ M^{-1}\ s^{-1}$ and a dissociation rate constant of $k_{off} = 3.58 \times 10^{-4}\ s^{-1}$. The rate constants appear to be within the same order of magnitude as those obtained from binding studies of radiolabeled huIL-4 to native receptor complexes in hematopoietic cell lines (Park et al., 1987; Cabrillat et al., 1987; Gallizi et al., 1989). However, a close evaluation of the two binding phenomena revealed notable differences. The calculated dissociation constant for huIL-4/shuIL-4Rα interaction ($K_d = 46$ pM) should be compared with current estimates of the dissociation constant for the interaction of radiolabeled huIL-4 and native receptors in responsive cell lines ($K_d \sim 75-205$ pM). Similarly, it should be contrasted with the affinity of radiolabeled huIL-4 for recombinant shuIL-4Rα overexpressed in COS-7 alone ($K_d = 266$ pM) or in combination with the γ-subunit of the huIL-2 receptor ($K_d = 79$ pM) (Russell et al., 1993). The relatively higher affinity observed in our system appears to confirm current concerns about the use of tyrosine iodination in the radiolabeling of huIL-4 for binding studies. It was postulated that radioiodination of the two tyrosine residues in huIL-4 could lead to a decrease in the binding affinity for functional receptors in cells (Zurawski et al., 1993). SPR analysis of the binding of huIL-4 to immobilized shuIL-4Rα also revealed that its dissociation kinetics was not biphasic and lacked the slow dissociating component which is characteristic of the dissociation of radiolabeled huIL-4 from cell surface receptors. Affinities of huIL-4 determined from binding studies with cells were probably underestimated since the slow dissociating component was not taken into account in the determination of rate constants. Taken together, the data suggest that the true affinity of huIL-4 for the native receptor complex could be higher than current estimates.

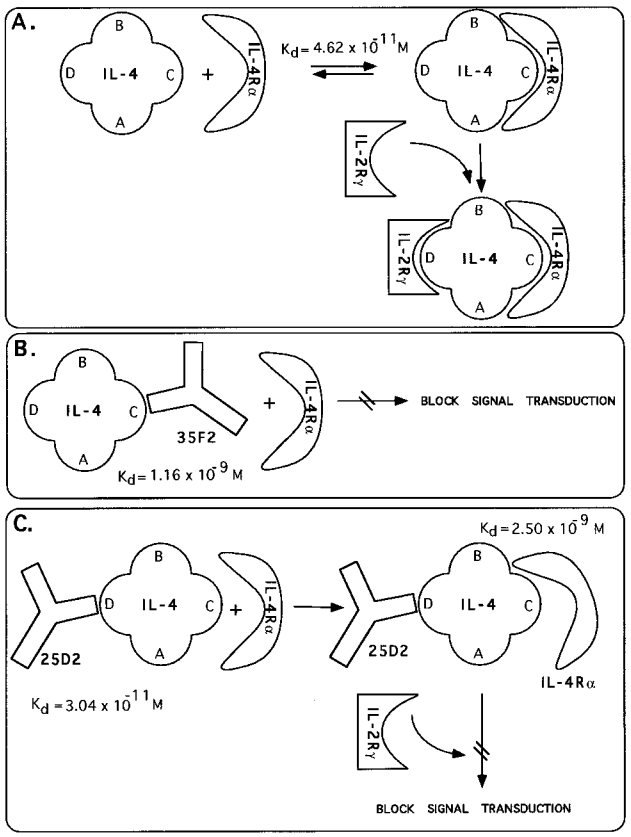

FIGURE 8: Model for the blocking activity of Mab 35F2 and Mab 25D2. (A) huIL-4 is represented by a cartoon exhibiting four α-helices A, B, C, and D available for interaction with functional receptors. The available evidence supports huIL-4Rα interaction with helix C and part of helix A of huIL-4. IL-2Rγ would recognize structural elements in helix D, especially near Y124. (B) Mab 35F2 excludes huIL-4 interaction with huIL-4Rα by binding to helix C. (C) Mab 25D2 binds to helix D of huIL-4 and decreases its affinity for huIL-4Rα by 54-fold in addition to excluding the putative binding of IL-2Rγ to helix D.

Surface plasmon resonance studies with the neutralizing monoclonal antibodies, 35F2 and 25D2, revealed a significant difference in their binding affinities for huIL-4. Real-time interaction experiments showed that the dissociation of huIL-4 from Mab 25D2 was 100-fold slower than from Mab 35F2 (Table 1). The calculated dissociation constant of Mab 35F2 ($K_d = 1.16 \times 10^{-9}$ M) was practically identical to the dissociation constant obtained previously in equilibrium binding studies using radiolabeled huIL-4. In contrast, the calculated dissociation constant of Mab 25D2 was notably smaller ($K_d = 3.04 \times 10^{-11}$ M). Previous K_d determinations for Mab 25D2 were based on equilibrium binding and immunoprecipitation techniques and consistently resulted in apparent K_d values in the nanomolar range (Ramanathan et al., 1991, 1993). This apparent lower affinity could be due to selective modification of critical lysines in the radiolabeled huIL-4 employed in the binding studies. Indeed, three lysine residues in huIL-4 (K_{117}, K_{123}, and K_{126}) reside within the epitope of Mab 25D2. In previous studies, the epitopes of Mabs 25D2 and 35F2 have been mapped to distinct sites on helices D and C, respectively, in huIL-4 (Ramanathan et al., 1993).

Studies of the effect of the antibodies on the binding of huIL-4 to shuIL-4Rα provided further insight about their mode of action (Figure 8). Mab 35F2 and shuIL-4Rα were mutually exclusive in their binding to huIL-4, as shown by

size exclusion chromatography of the mixture of all three components (Figure 4B). No ternary complex of huIL-4, Mab 35F2, and shuIL-4Rα was evident as it was in the mixture of Mab 25D2, huIL-4, and shuIL-4Rα chromatographed by size exclusion chromatography. These results were confirmed by binding studies in real time. Preincubation of huIL-4 with Mab 35F2 completely inhibited huIL-4 binding to shuIL-4Rα immobilized on a sensor chip (Figure 6). It is apparent that shuIL-4Rα and Mab 35F2 share a common epitope located within helix C of huIL-4. In support of this hypothesis, mutagenesis studies have implicated several residues in helix C (i.e. K_{84}, D_{87}, R_{88}, and N_{89}) as being essential for receptor binding and T cell proliferation activity (Ramanathan et al., 1993). In particular, R_{88} was identified as one of two key residues in huIL-4 that are essential for interaction with shuIL-4Rα. Mutation of R_{88} to Q or E diminished the affinity of the mutants by more than 1000-fold (Kruse et al., 1993).

Studies with Mab 25D2 revealed that it neutralized the activity of huIL-4 through a mechanism which is quite distinct from that of Mab 35F2. Binding of Mab 25D2 reduced the affinity of huIL-4 for shuIL-4Rα by 54-fold as shown in Table 1. The complex of Mab 25D2 and huIL-4 retained residual binding activity and interacted with shuIL-4Rα with a dissociation constant in the nanomolar range (K_d = 2.9 nM). The existence of a ternary complex of Mab 25D2, huIL-4, and shuIL-4Rα was demonstrated in size exclusion chromatography experiments and in real-time binding studies (Figures 4A and 6). These observations are consistent with the assignment of domains, in helices A and C, as the binding sites for shuIL-4Rα (Kruse et al., 1993). These domains in the three-dimensional structure of huIL-4 are sufficiently distinct from the epitope of Mab 25D2 which was mapped to residues 104−129 (β-strand 2 and helix D). Minor overlapping of these binding domains or small conformation changes in huIL-4 induced by the binding of Mab 25D2 would account for the diminished affinity for the shuIL-4Rα. The neutralization effect of Mab 25D2 may be explained by its interaction with helix D in huIL-4 (Ramanathan et al., 1993). This domain has been implicated in the recognition of a secondary receptor subunit which is essential for huIL-4 receptor function (Kruse et al., 1993). It was recently proposed that IL-2Rγ is the component of the huIL-4 receptor complex that recognizes helix D in huIL-4 (Reusch et al., 1994). In summary, the available evidence indicates that Mab 25D2 exerts its neutralization effect through a dual mechanism affecting the function of two receptor subunits simultaneously. In studies with a panel of seven mouse monoclonal antibodies, Reusch et al. (1994) have also identified several antibodies (3VD4, 4D9, and 8F12) which seem to neutralize the activity of huIL-4 by recognizing a domain within helix D. It would be of interest to further characterize these antibodies and contrast their mode of action with that of Mab 25D2, especially with regard to the binding of huIL-4 to the known subunits of the receptor complex.

Elucidation of the precise mechanism of neutralization by anti-cytokine antibodies, in conjunction with the characterization of the interaction of huIL-4 with shuIL-4Rα presented in this paper, provides a rational basis for the selection of these antibodies as candidates for humanization and clinical applications. These antibodies have potential utility as antagonists (Abrams et al., 1993) or as carriers in controlled release formulations (Fernandez-Botran & Vitetta, 1991; Finkelman et al., 1993; Sato et al., 1993; Maliszewski et al., 1994). The results of our studies further validate the use of neutralizing monoclonal antibodies in mapping functional receptor sites of cytokines. Information gained in these studies will become especially useful in the analysis of the three-dimensional structure of the multisubunit receptor/ligand complex determined by conventional X-ray crystallography or NMR methods.

ACKNOWLEDGMENT

We thank Schering-Plough Biotechnology Development for providing recombinant huIL-4 and the Mab 25D2 which were both essential for this study. We gratefully acknowledge Dr. G. F. Seelig's contribution to this effort, providing rabbit antisera (P71) to shuIL-4Rα. We also thank and acknowledge Dr. Ramanathan, who made an important contribution by providing Mab 35F2. In addition, we are grateful to Dr. P. C. Weber for critically reviewing the manuscript. Finally, this work would not have been possible without the dedication of many staff members of DNAX Research Institute & Schering-Plough France in cloning huIL-4, shuIL-4Rα, and the monoclonal antibodies 35F2 and 25D2.

REFERENCES

Abrams, J. S., Chretien, I., Lee, F. D., & Pearce, M. K. (1991) U.S. Patent 5,041,381.

Abrams, J. S., Dalie, B., Le, H. V., Miller, K., Murgolo, N. J., Nguyen, H., Pearce, M., Tindall, S., & Zavodny, P. J. (1993) *PCT, International Publication W093/17106*.

Bazan, J. F. (1990) *Proc. Natl. Acad. Sci. U.S.A. 87*, 6934−6938.

Cabrillat, H., Galizzi, J. P., Djossou, O., Arai, N., Yokota, T., Arai, K., & Banchereau, J. (1987) *Biochem. Biophys. Res. Commun. 149*, 995−1001.

Cook, W. J., Ealick, S. E., Reichert, P., Hammond, G., Le, H. V., Nagabhushan, T. L., Trotta, P. P., & Bugg, C. E. (1991) *J. Mol. Biol. 218*, 675−678.

Defrance, T., Vanbervliet, B., Aubry, J.-P., Takebe, Y., Arai, N., Miyajima, A., Yokota, T., Lee, F., Arai, K., De Vries, J. E., & Banchereau, J. (1987a) *J. Immunol. 139*, 1335−1141.

Defrance, T., Aubry, T. P., Rousset, F., Vanbervliet, B., Bonnefoy, J.-Y., Arai, N., Takebe, Y., Yokota, T., Lee, F., Arai, K., DeVries, J., & Banchereau, J. (1987b) *J. Exp. Med. 165*, 1459−1467.

DeKruyff, R. H., Turner, T., Abrams, J. S., Palladino, M. A., Jr., & Umetsu, D. T. (1989) *J. Exp. Med. 170*, 1477−1493.

Fägerstam, L. (1991) *Techniques in Protein Chemistry II*, pp 65−71, Academic Press, New York.

Fernandez-Botran, R., & Vitetta, E. S. (1991) *J. Exp. Med. 174*, 673−681.

Finkelman, F. D., Madden, K. B., Morris, S. C., Holmes, J. M., Boiani, N., Katona, I. M., & Maliszewski, C. R. (1993) *J. Immunol. 151*, 1235−1244.

Galizzi, J.-P., Zuber, C. E., Cabrillat, H., Djossou, O., & Banchereau, J. (1989) *J. Biol. Chem. 264*, 6984−6989.

Galizzi, J.-P., Zuber, C. E., Harada, N., Gorman, D. M., Djossou, O., Kastelein, R., Banchereau, J., Howard, M., & Miyajima, A. (1990) *Int. Immuno. 2*, 669−675.

Garrett, D. S. Powers, R., March, C. J., Frieden, E. A., Clore, G. M., & Gronenborn, A. M. (1992) *Biochemistry 31*, 4347−4353.

Hoffman, R. C., Castner, B. J., Gerhart, M., Gibson, M. G., Rasmussen, B. D., March, C. J., Weatherbee, J., Tsang, M., Gustchina, A., Schalk-Hihi, C., Reshetnikova, L., & Wlodawer, A. (1995) *Protein Sci. 4*, 382−386.

Izerda, R. L., March, C. J., Mosley, B., Lyman, S. D., Vanden Bos, T., Gimpel, S. D., Din, W. S., Grabstein, K. H., Widmer, M. B., Park, L. S., Cosman, D., & Beckmann, M. P. (1990) *J. Exp. Med. 171*, 861−873.

Johnsson, B., Löfås, S., & Lindqvist, G. (1991) *Anal. Biochem. 198*, 268−277.
Karlsson, R., Michaelsson, A., & Mattsson, L. (1991) *J. Immunol. Methods 145*, 229−240.
Kondo, M., Takeshita, T., Ishii, N., Nakamura, M., Watanabe, S., Arai, K., & Sagamura, K. (1993) *Science 262*, 1874−1877.
Kruse, N., Shen, B.-J., Arnold, S., Tony, H.-P., Müller, T., & Sebald, W. (1993) *EMBO J. 12*, 5121−5129.
Le, H. V., Ramanathan, L., Labdon, J. E., Mays-Ichinco, C., Syto, R., Arai, N., Hoy, P., Takebe, Y., Nagabhushan, T. L., & Trotta, P. P. (1988) *J. Biol. Chem. 263*, 10817−10823.
Le, H. V., Seelig, G. F., Syto, R., Ramanathan, L., Windsor, W., Borkowski, D., & Trotta, P. P. (1991) *Biochemistry 30*, 9576−9582.
Little, J. R., & Donahue, H. (1967) in *Methods in Immunology and Immunochemistry* (Williams, C. A., & Chase, M. A., Eds.) Vol. 2, p 343, Academic Press, New York.
Littman, B. H., Dastvan, F. F., Carlson, P. L., & Sanders, K. M. (1989) *J. Immunol. 142*, 520−525.
Maliszewski, C. R., Sato, T. A., Davison, B., Jacobs, C. A., Finkelman, F. D., & Fanslow, W. C. (1994) *Proc. Soc. Exp. Biol. Med. 206*, 233−237.
Mosmann, T. R., Bond, M. W., Coffman, R. L., Ohara, J., & Paul, W. E. (1986) *Proc. Natl. Acad. Sci. U.S.A. 83*, 5654.
Park, L., Friend, D., Sassenfeld, H., & Urdal, D. (1987) *J. Exp. Med. 166*, 476.
Paul, W. E. (1991) *Blood 77*, 1859−1870.
Pene, J., Rousset, F., Briere, F. Chretien, I., Bonnefoy, J.-Y., Spits, H., Yokota, T., Arai, N., Arai, K.-I., & Banchereau, J. (1998) *Proc. Natl. Acad. Sci. U.S.A. 85*, 6880−6884.
Powers, R., Garrett, D. S., March, C. J., Frieden, E. A., Gronenborn, A. M., & Clore, G. M. (1992b) *Science 256*, 1673−1677.
Rajan, N., Tsarbopoulos, A., Kumarasamy, R., O'Donnell, R., Taremi, S. S., Baldwin, S. W., Seelig, G. F., Fan, X., Pramanik, B., & Le, H. V. (1995) *Biochem. Biophys. Res. Commun. 206*, 694−702.
Ramanathan, L., Ingram, R., Abrams, J., Payvandi, F., Trotta, P. P., & Le, H. V. (1990) in *Advances in Gene Technology: The Molecular Biology of Immune Diseases and the Immune Response* (Streilein, J. W., et al., Eds.) p 163, IRL Press, Oxford.
Ramanathan, L., Ingram, R., Sullivan, L., Greenberg, R., Reim, R., Trotta, P. P., & Le, H. V. (1993) *Biochemistry 32*, 3549−3556.
Reusch, P., Arnold, S., Heusser, C., Wagner, K., Weston, B., & Sebald, W. (1994) *Eur. J. Biochem. 222*, 491−499.
Rousset, F., De Waal Malefyt, R., Slierendregt, B., Aubry, P., Bonnefoy, J.-Y., Defrance, T., Banchereau, J., & de Vries, J. (1988) *J. Immunol. 140*, 2625−2632.
Russell, S. M., Keegan, A. D., Harada, N., Nakamura, Y., Noguchi, M., Leland, P., Friedmann, M. C., Miyajima, A., Puri, R. K., Paul, W. E., & Leonard, W. J. (1993) *Science 262*, 1880−1883.
Sato, T. A., Widmer, M. B., Finkelman, F. D., Madani, H., Jacobs, C. A., Grabstein, K. H., & Maliszewski, C. R. (1993) *J. Immunol. 150*, 2717−2723.
Smith, L. J., Redfield, C., Boyd, J., Lawrence, G. M. P., Edwards, R. G., Smith, R. A. G., & Dobson, C. M. (1992) *J. Mol. Biol. 224*, 899−904.
Spits, H., Yssel, H., Takebe, Y., Arai, N., Yokota, T., Lee, F., Arai, K., Banchereau, J., & de Vries, J. (1987) *J. Immunol. 139*, 1142−1147.
Stenberg, E., Persson, B., Ross, H., & Urbaniczky, C. (1991) *J. Colloid Interface Sci. 143*, 513−526.
Takeshita, T., Asao, H., Ohtani, K., Ishii, N., Kumaki, S., Tanaka, N., Munakata, H., Nakamura, M., & Sagamura, K. (1992) *Science 257*, 379−382.
Tang, J. C. T., Naveh, D., & Nagabhushan, T. L. (1991) U.S. Patent 5,077,388.
Taremi, S. S., Prosise, W. W., Rajan, N., Seelig, G. F., Trotta P. P., Nagabhushan, T. L., & Le, H. V. (1993) *Protein Sci. 2* (Suppl. 1), 114.
te Velde, A. A., Klomp, J. P.-G., Yard, B. A., deVries, J. E., & Figdor, C. G. (1988) *J. Immunol. 142*, 520−525.
Walter, M. R., Cook, W. J., Zhao, B. G., Cameron, R., Ealick, S. E., Walter, R. L., Reichert, P., Nagabhushan, T. L., Trotta, P. P., & Bugg, C. E. (1992) *J. Biol. Chem. 267*, 20371−20376.
Windsor, W. T., Syto, R., Le, H. V., & Trotta, P. P. (1991) *Biochemistry 30*, 1259−1264.
Wlodawer, A., Pavlovsky, A., & Gustchina, A. (1992) *FEBS Lett. 309*, 59−64.
Zurawski, S. M., Vega, F., Huyghe, B., & Zurawski, G. (1993) *EMBO J. 12*, 2663−2670.

BI951741T